JB
Journals.ASM.org

Defect in the Formation of 70S Ribosomes Caused by Lack of Ribosomal Protein L34 Can Be Suppressed by Magnesium

Genki Akanuma,[a] Ako Kobayashi,[a] Shota Suzuki,[b]* Fujio Kawamura,[b]* Yuh Shiwa,[c] Satoru Watanabe,[d] Hirofumi Yoshikawa,[c,d] Ryo Hanai,[b] Morio Ishizuka[a]

Department of Applied Chemistry, Faculty of Science and Engineering, Chuo University, Tokyo, Japan[a]; Department of Life Science and Research Center for Life Science, College of Science, Rikkyo University, Tokyo, Japan[b]; Genome Research Center, NODAI Research Institute, Tokyo University of Agriculture, Tokyo, Japan[c]; Department of Bioscience, Tokyo University of Agriculture, Tokyo, Japan[d]

To elucidate the biological functions of the ribosomal protein L34, which is encoded by the *rpmH* gene, the *rpmH* deletion mutant of *Bacillus subtilis* and two suppressor mutants were characterized. Although the Δ*rpmH* mutant exhibited a severe slow-growth phenotype, additional mutations in the *yhdP* or *mgtE* gene restored the growth rate of the Δ*rpmH* strain. Either the disruption of *yhdP*, which is thought to be involved in the efflux of Mg^{2+}, or overexpression of *mgtE*, which plays a major role in the import of Mg^{2+}, could suppress defects in both the formation of the 70S ribosome and growth caused by the absence of L34. Interestingly, the Mg^{2+} content was lower in the Δ*rpmH* cells than in the wild type, and the Mg^{2+} content in the Δ*rpmH* cells was restored by either the disruption of *yhdP* or overexpression of *mgtE*. *In vitro* experiments on subunit association demonstrated that 50S subunits that lacked L34 could form 70S ribosomes only at a high concentration of Mg^{2+}. These results showed that L34 is required for efficient 70S ribosome formation and that L34 function can be restored partially by Mg^{2+}. In addition, the Mg^{2+} content was consistently lower in mutants that contained significantly reduced amounts of the 70S ribosome, such as the Δ*rplA* (L1) and Δ*rplW* (L23) strains and mutant strains with a reduced number of copies of the *rrn* operon. Thus, the results indicated that the cellular Mg^{2+} content is influenced by the amount of 70S ribosomes.

The eubacterial ribosome (70S), which plays a central role in protein synthesis, is composed of a small (30S) subunit and a large (50S) subunit. The small subunit is comprised of the 16S rRNA and more than 20 proteins, whereas the large subunit is comprised of the 23S and 5S rRNAs and more than 30 proteins (1, 2). The molecular mechanisms of translation have been elucidated in detail by the convergence of various approaches, including crystal structure analysis (3–8). The individual functions of several ribosomal proteins have also been elucidated by biochemical and genetic analyses, including reconstitution and mutational analysis. For example, ribosomal protein L2 plays important roles in the assembly of the ribosomal subunits, binding of the tRNA to the A and P sites, peptidyltransferase activity, and formation of the peptide bond (9–13). However, in general, disruption of the genes that encode the ribosomal proteins has been avoided as a means of identifying protein function, because these genes, which are highly conserved in bacteria, have been considered essential for cell proliferation (14). Nonetheless, recently, it was found that 22 of the 54 *Escherichia coli* genes for ribosomal proteins could be deleted on an individual basis (15, 16). We have also shown that out of the 57 ribosomal-protein-encoding genes that have been annotated in the Gram-positive bacterium *Bacillus subtilis*, at least 22 genes are not individually essential for cell proliferation (17). The *rpmH* gene encoding ribosomal protein L34, which is a component of the large subunit, is one of the genes that can be disrupted. Lack of L34 causes a severe defect in the formation of the 70S ribosome and a reduced growth rate (17). The *rpmH* genes of many bacteria were cloned over 2 decades ago by researchers working on replication initiation, because the gene is located near the replication origin in many bacteria (18–22). It is known that L34 assembles into the 50S subunit at a late stage of its formation (23), and it has also been suggested that L34 participates in the regulation of the polyamine biosynthetic pathway (24). However, the functions of L34 within the ribosome, such as its involvement in protein synthesis, large subunit assembly, and 70S formation, remain unclear.

Magnesium is important for the maintenance of ribosome structure and for translation. The *in vitro* association of the 30S and 50S ribosomal subunits to form intact 70S ribosomes depends strongly on the concentration of Mg^{2+} ions within the cell (25–27). Mg^{2+} is also required for both stabilization of the secondary structure of rRNA and binding of the ribosomal proteins to the rRNA (28–30). Furthermore, Mg^{2+} stabilizes the codon-anticodon interaction in the A site and influences the binding of ribosome recycling factor (RRF) to the ribosome (31–34). In addition to its involvement in the ribosome, Mg^{2+} has a crucial role in numerous biological processes and cellular functions, such as the activation and catalytic reactions of hundreds of enzymes, utilization of ATP, and maintenance of genomic stability (35, 36).

In the present study, we isolated two suppressor mutants, the Δ*rpmH srh1* and Δ*rpmH srh2* mutants, from the Δ*rpmH* mutant strain and characterized these mutants to elucidate the biological functions of the ribosomal protein L34 in *B. subtilis*. The studies

Received 5 June 2014 **Accepted** 23 August 2014

Published ahead of print 2 September 2014

Address correspondence to Genki Akanuma, akanuma@kc.chuo-u.ac.jp.

* Present address: Shota Suzuki, Department of Biotechnology, Graduate School of Agriculture and Life Sciences, The University of Tokyo, Tokyo, Japan; Fujio Kawamura, Department of Bioscience, Tokyo University of Agriculture, Tokyo, Japan.

Supplemental material for this article may be found at http://dx.doi.org/10.1128/JB.01896-14.

doi:10.1128/JB.01896-14

on the suppression mechanism of the *srh1* and *srh2* suppressor mutations indicated that the function of L34, which is involved not only in normal assembly of the 50S subunit but also in efficient formation of the 70S ribosome, can be complemented partially by Mg^{2+} ions. Furthermore, we found that the content of Mg^{2+} in the cell is influenced by the amount of 70S ribosomes. On the basis of our findings, we also discuss the importance of Mg^{2+} ions in the ribosome.

MATERIALS AND METHODS

Media and culture conditions. LB medium (37) and LB agar were used. The culture conditions and media for preparing competent cells have been described previously (38). When required, 0.5 μg ml^{-1} erythromycin, 5 μg ml^{-1} kanamycin, 1 mM isopropyl-β-D-thiogalactopyranoside (IPTG), and 100 mM or 200 mM $MgSO_4$ were added to the medium. Ampicillin (50 μg ml^{-1}) was used to select *E. coli* strains. To observe growth under Mg^{2+}-deficient conditions, cells were grown in minimal medium with Casamino Acids (MCA medium) that contained 1 mM $MgSO_4$ at 37°C with shaking to early exponential phase (optical density at 600 nm [OD_{600}] of ~0.2) and harvested. The harvested cells were washed with MCA medium without $MgSO_4$, reinoculated into MCA medium that contained 1 mM or 10 μM $MgSO_4$, and grown at 37°C with shaking. MCA medium is based on Spizizen's minimal glucose medium (39). The composition of MCA medium is as follows: 6 g of KH_2PO_4, 14 g of K_2HPO_4, 2 g of $(NH_4)_2SO_4$, 1 g of trisodium citrate · $2H_2O$ per liter of distilled and deionized water, 0.5% glucose, and 0.1% Casamino Acids (Difco). It should be noted that 0.1% Casamino Acids is equivalent to 6 μM Mg^2.

Bacterial strains and plasmids. All the *B. subtilis* strains used in the study were isogenic with *B. subtilis* strain 168 *trpC2*. The Δ*rpmH*::*cat* strain, which was constructed by replacing the open reading frame of the *rpmH* gene with a *cat* gene that lacked any promoter or Rho-independent terminator sequence, was described previously (17). The plasmid pDGrpmH, which carries an *rpmH* gene controlled by an IPTG-inducible Pspac promoter, was constructed as follows. The *rpmH* gene and the terminator region of the *rpmE* gene were amplified using the primers rpmHF and rpmHR and primers rpmEterF and rpmEterR, respectively (see Table S1 in the supplemental material for the nucleotide sequences of all the primers used in this study). These fragments were then used simultaneously as the template for PCR amplification with the primers rpmHF and rpmEterR. The resulting fragment was digested with HindIII and SalI and cloned into pDG148 (40). The plasmid pDGyhdP, which carries the *yhdP* gene controlled by an IPTG-inducible Pspac promoter, was constructed as follows. The *yhdP* gene and the terminator region of the *rpmE* gene were amplified using the primers yhdPF and yhdPR and primers rpmEterFYP and rpmEterR2, respectively. These fragments were then used simultaneously as the template for PCR amplification with the primers yhdPF and rpmEterR2. The resulting fragments were digested with SalI and SphI and cloned into pDG148. Similarly, to construct the plasmid pDGmgtE, which carries the *mgtE* gene without a riboswitch (41) controlled by the Pspac promoter, the *mgtE* gene and the terminator region of the *rpmE* gene were amplified using the primers mgtEF and mgtER and primers rpmEterFME and rpmEterR2, respectively. These fragments were then used simultaneously as the template for PCR amplification with primers yhdPF and rpmEterR2. The resulting fragments were digested with SalI and SphI and cloned into pDG148. To replace the *yhdP* gene with an erythromycin resistance gene (*erm*), oligonucleotide primers were used to amplify the upstream (yhdPuF and yhdPuR) and downstream (yhdPdF and yhdPdR) regions of the *yhdP* gene. Next, the *erm* gene of pTC3 (formally named pAE41 [42]) was amplified by PCR using the primers ermF and ermR. Another PCR amplification, in which all three above-mentioned amplified fragments were added as the DNA template, was performed using the primers yhdPuF and yhdPdR. The resulting fragment was used to transform strain 168 (*trpC2*), giving rise to the erythromycin-resistant transformant (Δ*yhdP*::*erm trpC2*). Chromosomal DNA extracted from the Δ*rpmH*::*cat* mutant was used to transform the Δ*yhdP*::*erm* strain, and the transformants were selected on the basis of a chloramphenicol-resistant phenotype (Δ*rpmH*::*cat* Δ*yhdP*::*erm trpC2*). The strain whose genome encoded MgtE tagged with Strep-tag II (WSH PQFEK) was constructed as follows. The region upstream of the *aprE* gene was amplified with the primers aprEUF and aprEURmg and the region downstream was amplified with the primers aprEDF and aprEDR using chromosomal DNA from *B. subtilis* strain 168 as the template. The *mgtE* gene, including the promoter and riboswitch, was amplified with primers mgtEstF and mgtEstR, which also encoded the Strep-tag II, using chromosomal DNA from strain 168 as the template. The kanamycin resistance gene from pDG148 was amplified by PCR using the primers kanF and kanR. The four fragments obtained (i.e., the upstream and downstream regions of *aprE* [fragments A and B, respectively] and the *mgtE* region and the kanamycin resistance gene [fragments C and D, respectively]) were used as the templates for two rounds of PCR amplification. First, fragments A and C were used simultaneously as the templates for amplification with primers aprEUF and mgtEstR, and fragments B and D were used simultaneously as the templates for amplification with primers kanF and aprEDR. Next, the two fragments obtained were used simultaneously as the templates for amplification with primers aprEUF and aprEDR. Finally, the resulting product was used to transform strain 168, and kanamycin-resistant transformants were selected (*aprE*::*mgtE-Streptag kan trpC2*). Chromosomal DNA extracted from the Δ*rpmH*::*cat* strain was used to transform the *aprE*::*mgtE-Streptag kan* mutant, and the transformants were selected on the basis of a chloramphenicol-resistant phenotype (Δ*rpmH*::*cat aprE*::*mgtE-Streptag kan trpC2*). Strains whose genomes encoded YhdP tagged with the Strep-tag II in the wild-type background (*aprE*::*yhdP-Streptag kan trpC2*) or in the Δ*rpmH* background (Δ*rpmH*::*cat aprE*::*yhdP-Streptag kan trpC2*) were constructed in a similar manner. The region upstream of the *aprE* gene was amplified with the primers aprEUF and aprEURyh, and the region downstream was amplified with the primers aprEDF and aprEDR. The *yhdP* gene, including the promoter, was amplified with the primers yhdPstF and yhdPstR. The kanamycin resistance gene was amplified by PCR using the primers kanF and kanR.

Isolation and identification of suppressor mutations in the Δ*rpmH* mutant. To obtain spontaneous suppressor mutations in the Δ*rpmH* mutant that restored growth, an overnight culture of the Δ*rpmH* strain was diluted and plated onto LB solid medium and then incubated overnight at 37°C. Two suppressor mutants that formed larger colonies than did the parental strain were designated the Δ*rpmH srh1* and Δ*rpmH srh2* mutants. The Δ*rpmH srh1* colonies were larger than those of the Δ*rpmH* parental strain but smaller than those of the Δ*rpmH srh2* strain. The Δ*rpmH srh2* colonies were almost the same size as those of the wild type. The frequency of Δ*rpmH srh1*-type suppressor mutants was 0.16%, whereas the frequency of Δ*rpmH srh2*-type mutants was 0.006%. To identify the suppressor mutations, sequencing libraries were prepared using the NEBNext DNA Sample Prep reagent set 1 (New England BioLabs) according to the manufacturer's protocols. Briefly, 3 μg of genomic DNA was fragmented to an average length of 300 bp using the Covaris S2 system (Covaris, Woburn, MA). The fragmented DNA was repaired, a single A nucleotide was ligated to the 3′ end, Illumina Index PE adapters (Illumina, San Diego, CA) were ligated to the fragments, and fragments between 350 and 450 bp were selected with a 1.5% Pippin Prep gel (Sage Science, Beverly, MA). The size-selected sample was amplified by PCR for 12 cycles with the primers InPE1.0, InPE2.0, and an index primer, which contained a unique-index tag for each individual sample. The final product was validated by using an Agilent Bioanalyzer 2100 (Agilent, Santa Clara, CA). The pooled libraries were sequenced on an Illumina Genome Analyzer IIx in accordance with the manufacturer's instructions, to generate 100-bp paired-end reads and 6-bp index tags. Details of the output data are given in Table S2 in the supplemental material. Sequence reads from each sample were mapped onto the *B. subtilis* 168 reference genome (accession no. NC_000964.3), using the BWA software package (ver. 0.5.1) (44) with default parameters. Possible variations (single nucleotide polymorphism [SNP]/indel) were listed using the SAMtools software (ver. 0.1.9) (43). To

identify authentic variations, we applied the following filtering criteria to the candidates: (i) coverage at the nonreference allele of at least 5, (ii) indels had to meet an SNP quality threshold of 50 and substitutions had to meet an SNP quality threshold of 20 (SAMtools assigns SNP quality, which is the Phred-scaled probability that the consensus is identical to the reference), (iii) variations had to meet a mapping quality of 30 (SAMtools assigns mapping quality, which is the Phred-scaled probability that the read alignment is wrong), and (iv) percentage of sequence reads showing the variant allele had to exceed 55%. The filtered lists of variations were annotated by COVA (comparison of variants and functional annotation) (http://sourceforge.net/projects/cova/). To identify structural variations, we used the BreakDancer software package (ver. 0.0.1r81) (45) with default parameters. Regions of interest were inspected on the Integrative Genomics Viewer (IGV) (46).

Measurement of Mg^{2+} content in a cell. *Bacillus subtilis* cells were grown in LB medium at 37°C with shaking to exponential phase (OD_{600}, ~0.4) and harvested. Simultaneously, viable cells were counted by plating the culture on LB agar plates and then incubating them at 37°C for 24 h. The cells were resuspended in lysis buffer (10 mM Tris-HCl, pH 8.0, 1 mg ml^{-1} lysozyme) and disrupted sufficiently by sonication, and then the pH of the crude extract was adjusted to approximately 3.0 with hydrochloric acid in order to denature the proteins. After vortexing for 10 min followed by incubation at room temperature for 10 min, the crude extract was centrifuged for 10 min at 10,000 × *g*. The amount of Mg^{2+} in the supernatant was measured with a Metallo assay kit for magnesium (Metallogenics) in accordance with the manufacturer's instructions. The Mg^{2+} content per cell was calculated by dividing the amount of Mg^{2+} in the crude extract by the number of viable cells. The concentration of Mg^{2+} was calculated by assuming that a *B. subtilis* cell is a cylinder (radius, 0.4 μm; length, 4 μm).

Sucrose density gradient sedimentation analysis. *Bacillus subtilis* cells were grown in LB medium at 37°C with shaking to exponential phase (OD_{600}, ~0.4) and harvested. The sucrose density gradient sedimentation analysis was performed as described previously (47). Briefly, the cells were disrupted by passage through a French pressure cell and cell debris was removed by centrifugation. Aliquots of extract were layered onto 10 to 40% sucrose density gradients and centrifuged at 4°C for 17.5 h at 65,000 × *g* (Hitachi P40ST rotor). Samples were collected with a piston gradient fractionator (BioComP), and absorbance profiles were monitored at 254 nm using a Bio-Mini UV monitor (Atto, Japan). When normalizing the applied volume by the total absorbance at 260 nm, 10 A_{260} units of crude extract per tube were used (see Fig. 4). When normalizing the applied volume by the amount of chromosomal DNA (see Fig. 6B), chromosomal DNA was extracted from 1 ml of each culture that was used for density gradient sedimentation analysis and quantified by spectrophotometric assay. The OD_{600} of each sample was measured before (designated Db) and after (designated Da) passage through the French press, and the efficiency of cell lysis (designated *E*) for each sample was calculated from the following equation: $E = 1 - Da/Db$. The volume of wild-type extract used for the assay was determined by measuring the A_{260} of the extract obtained from the wild-type cells and calculating the volume of wild-type extract that contained 10 A_{260} units (designated A_{wt}). The volume of extract for each mutant to be used for the assay (designated A_{mut}) was determined from the following equation: $A_{mut} = A_{wt} \times (C_{wt} \times E_{wt})/(C_{mut} \times E_{mut})$, where C_{wt} and C_{mut} are the total amounts of chromosomal DNA extracted from the wild-type and mutant cells, respectively, and E_{wt} and E_{mut} are the efficiency of cell lysis for the wild-type and mutant cultures, respectively.

Analysis of 70S ribosome formation. 30S and 50S ribosomal subunits were prepared from wild-type and Δ*rpmH* mutant cells grown in LB at 37°C. The preparation of small and large subunits and association experiments were performed as described previously with a slight modification (48). Briefly, the S30 fraction prepared from wild-type cells cultivated to exponential phase (OD_{600}, ~0.4) was centrifuged at 65,000 × *g* at 4°C for 17 h through a 10 to 40% sucrose gradient in buffer B (20 mM Tris-HCl, pH 7.6, 100 mM CH_3COONH_4, 0.1 mM dithiothreitol [DTT], and 2 mM phenylmethylsulfonyl fluoride [PMSF]) that contained 1 mM $(CH_3COO)_2Mg$ in a Hitachi P28SA rotor to separate the 30S and 50S subunits. In the case of the S30 fraction prepared from Δ*rpmH* mutant cells cultivated to exponential phase (OD_{600}, ~0.4), buffer B that contained 10 mM $(CH_3COO)_2Mg$ was used but otherwise the centrifugation was carried out under the same conditions. The subunits were diluted (1:2) with buffer B that contained 10 mM $(CH_3COO)_2Mg$, sedimented at 65,000 × *g* for 21 h at 4°C in a Hitachi P40ST rotor, and suspended in buffer B that contained 10 mM $(CH_3COO)_2Mg$. The purified small subunits (A_{260} = 1) and large subunits (A_{260} = 2.5) were mixed in buffer B that contained an appropriate concentration of $(CH_3COO)_2Mg$ and incubated for 15 min at 37°C. The mixture was centrifuged at 55,000 × *g* for 17.5 h at 4°C through a 10 to 40% sucrose gradient in buffer B that contained an appropriate concentration of $(CH_3COO)_2Mg$ in a Hitachi P40ST rotor. Absorbance profiles were monitored at 254 nm using a piston gradient fractionator (Biocomp) and a Bio-Mini UV monitor (Atto).

Preparation of crude ribosomes and RFHR 2-D gel electrophoresis. Cells were grown in LB medium at 37°C and harvested in exponential phase (OD_{600}, ~0.4). Crude ribosomes were obtained as described previously (49). The radical free and highly reducing (RFHR) two-dimensional (2-D) gel electrophoresis (50) was performed essentially in accordance with the published procedures (49).

Western blot analysis. Aliquots (30 μg of protein) of crude extracts that had been prepared from cells were loaded onto a sodium dodecyl sulfate-polyacrylamide gel (12%) and transferred to a polyvinylidene difluoride (PVDF) membrane (Millipore). Strep-Tactin alkaline phosphatase (AP) conjugate (IBA), which can detect Strep-tag II fusion proteins, was used at a dilution of 1:4,000. Immunodetection procedures were carried out in accordance with the manufacturer's instructions.

Nucleotide sequence accession number. The raw sequence reads used in this study are available at the DDBJ Sequence Read Archive (DRA) under accession no. DRA002237.

RESULTS

Isolation of suppressor mutants from Δ*rpmH* and identification of the corresponding mutations. In the Δ*rpmH*::*cat* mutant, the growth rate was significantly lower than that in the wild type, which was mainly due to a defect in 70S ribosome formation followed by a reduction of translation activity in the cell (17) (Fig. 1; see also Fig. 4). To investigate the possibility that insertion of the *cat* gene into the *rpmH* gene, which is located near the replication origin, affects the growth rate by inhibiting the initiation of DNA replication, genetic complementation tests were performed. We expected the expression level of *rpmH* to be very high, because *rpmH* is located near the replication origin and encodes a ribosomal protein that is expressed abundantly in cells. Consequently, we introduced a multicopy plasmid that contained the *rpmH* gene under the control of an IPTG-inducible Pspac promoter into the Δ*rpmH* mutant to ensure a sufficiently high level of expression of *rpmH* in the complementation test. As expected, the induction of *rpmH* expression restored the growth rate of the Δ*rpmH* mutant to that of the wild type (Fig. 1). This result demonstrated that the severe slow-growth phenotype observed in the Δ*rpmH* mutant could be attributed solely to the lack of ribosomal protein L34.

Two suppressor mutants were isolated spontaneously from the Δ*rpmH* mutant strain and designated Δ*rpmH srh1* (suppressor of *rpmH*) and Δ*rpmH srh2*. The slow growth caused by lack of L34 was moderately corrected in the Δ*rpmH srh1* strain, whereas the Δ*rpmH srh2* mutant showed almost the same growth rate as that of the wild type (Fig. 2A). To identify the suppressor mutations,

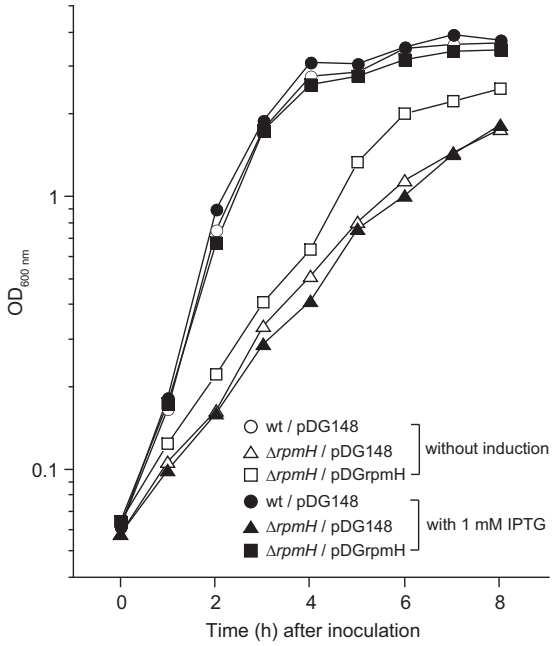

FIG 1 Genetic complementation of the Δ*rpmH* mutation. Cells were grown in LB at 37°C, and the optical density at 600 nm was measured. wt, wild type.

differences in sequence (SNP/indel mutations) between the Δ*rpmH* mutant, the Δ*rpmH srh1* or Δ*rpmH srh2* strain, and the *B. subtilis* 168 reference genome (accession no. NC_000964.3) were detected by whole-genome sequencing. When detected sequence differences in the suppressor mutants were compared with the sequence of the parental strain (Δ*rpmH*), it was apparent that the *yhdP* gene in the Δ*rpmH srh1* strain contained a 175-bp duplication, whereas the Δ*rpmH srh2* mutant harbored two nucleotide substitutions that converted Asp343 to Ala in the YhdP protein and Ala266 to Val in the MgtE protein (formerly called YkoK). It should be noted that no other changes in the genome were detected in the suppressor mutants. Given that the frequency of Δ*rpmH srh2*-type mutant colonies was much lower than that of Δ*rpmH srh1*-type mutant colonies (0.006% versus 0.016%), it is probable that Δ*rpmH srh2*-type mutant colonies arose from Δ*rpmH srh1*-type mutant strains through a second spontaneous mutation. YhdP shows homology with CorB and CorC of *Salmonella enterica* serovar Typhimurium (24% and 27% identity, respectively), which have been predicted to be efflux pumps for Mg^{2+} (51). Detailed studies on MgtE, including crystal structure analyses in *Thermus thermophilus*, have demonstrated that MgtE is an Mg^{2+} transporter that plays a central role in Mg^{2+} homeostasis (52–54). Recently, it has also been reported that MgtE in *B. subtilis*, which shows 33% sequence identity with MgtE of *T. thermophilus*, provides the primary route of magnesium import, although YfjQ, a homologue of the magnesium/cobalt transporter CorA, is also able to import Mg^{2+} (74).

Disruption of *yhdP* and overexpression of *mgtE* restored the reduction in the cellular Mg^{2+} content caused by lack of L34. To confirm that the mutations detected in the *yhdP* and *mgtE* genes did indeed suppress the defects observed in the Δ*rpmH* mutant, the *yhdP* and *mgtE* genes were each integrated into a multicopy plasmid separately, and the resulting plasmids were introduced into the Δ*rpmH* mutant. When these genes were induced in the absence of L34, overexpression of YhdP exacerbated the defect in the growth rate, whereas overexpression of MgtE partially restored the growth rate (Fig. 2B). This observation prompted us to disrupt *yhdP* in the Δ*rpmH* strain. As expected, elimination of YhdP in the Δ*rpmH* mutant partially restored the growth rate (Fig. 2B). Furthermore, when *yhdP* was disrupted and *mgtE* was over-

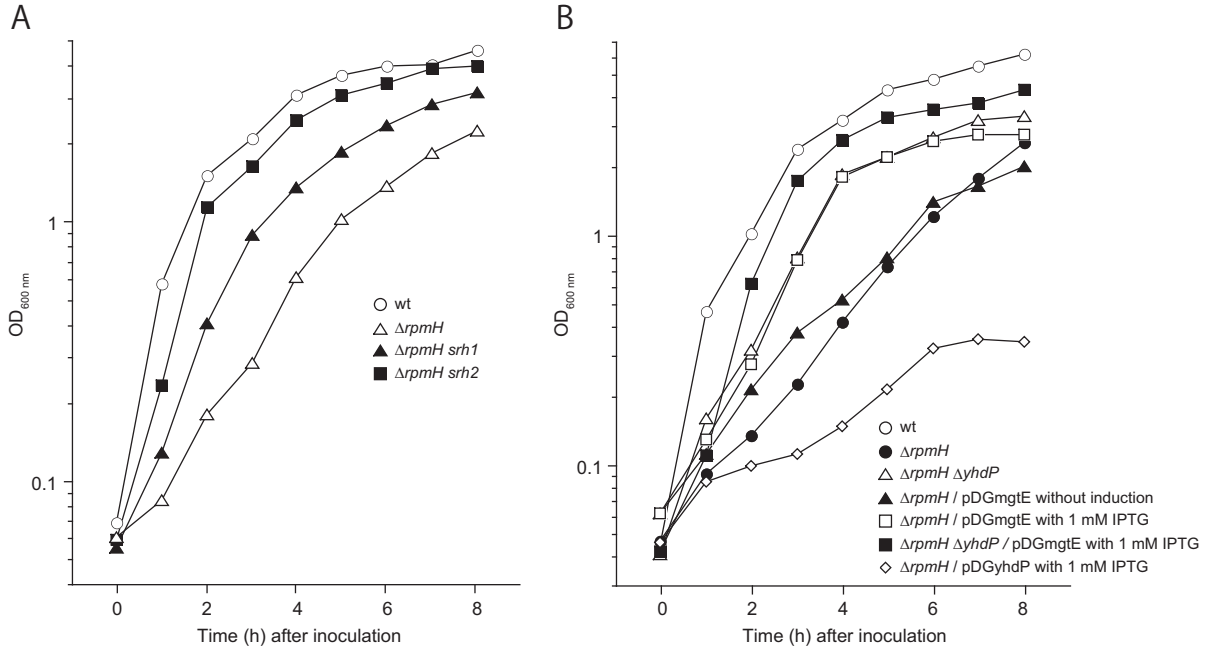

FIG 2 Suppression of the reduced growth rate observed in the Δ*rpmH* mutant. Cells were grown in LB at 37°C, and the optical density at 600 nm was measured. wt, wild type.

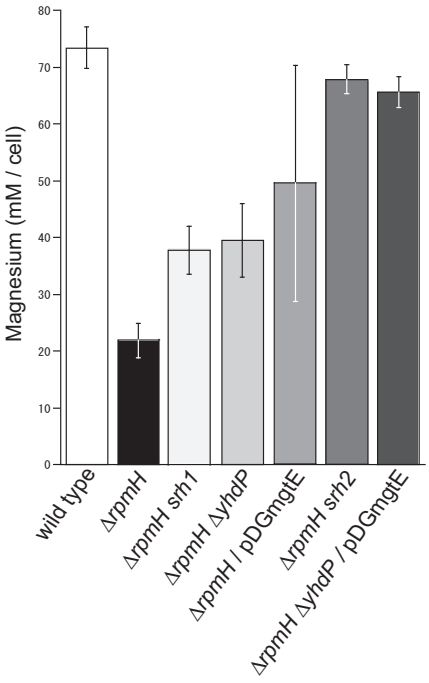

FIG 3 Observed reduction of Mg^{2+} content in the Δ*rpmH* cells and its restoration by the suppressor mutations as well as by disruption of *yhdP* and overexpression of *mgtE*. The Mg^{2+} contents per cell in exponential phase, which were measured as described in Materials and Methods, are shown. The term "/pDGmgtE" indicates the overexpression of *mgtE* in the mutant cells. The means of three independent experiments are shown. Error bars indicate standard deviations.

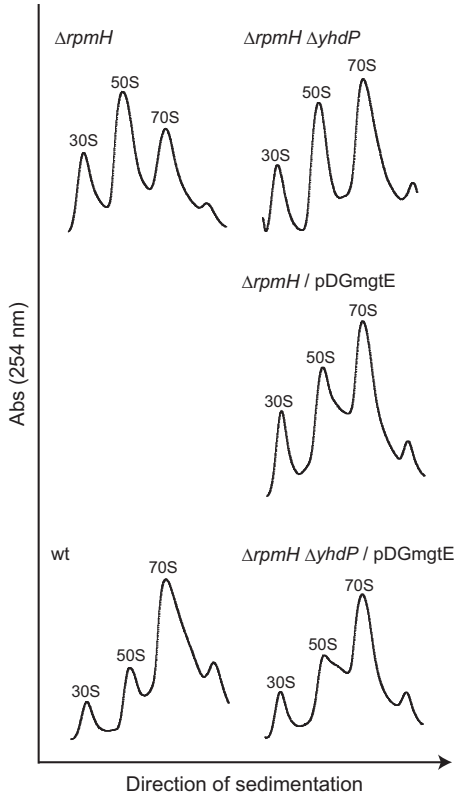

FIG 4 Defect in 70S ribosome formation in the absence of L34 and its suppression by the disruption of *yhdP* and overexpression of *mgtE*. Crude cell extracts were sedimented through a 10 to 40% sucrose gradient as described in Materials and Methods. The 30S, 50S, and 70S peaks are indicated in each individual profile. The term "/pDGmgtE" indicates the overexpression of *mgtE* in the mutant cells. wt, wild type; Abs, absorbance.

expressed simultaneously in the Δ*rpmH* strain, the growth rate was almost the same as that of the wild type (Fig. 2B). It should be noted that neither overexpression of *yhdP* or *mgtE* nor disruption of *yhdP* affected the growth of wild-type cells (see Fig. S1 in the supplemental material). In combination with the observations that overexpression of MgtE, a Mg^{2+} transporter, and disruption of YhdP, a homologue of the presumed Mg^{2+} efflux pumps CorB and CorC, restored the growth rate of the Δ*rpmH* mutant, these data strongly suggested that increasing the cellular Mg^{2+} concentration suppresses the defects caused by the lack of L34. To test this hypothesis, the Mg^{2+} content in the mutants and wild-type cells was determined using xylidyl blue I, which forms a chelate complex with Mg^{2+}. The Mg^{2+} ions that were chelated in enzymes and ribosomes were probably also detected by this method, because the cells were disrupted sufficiently by sonication and proteins were denatured by acid treatment, as described in Materials and Methods. Figure 3 shows the amount of Mg^{2+} per cell in the wild type and in each mutant. The concentration of Mg^{2+} in a wild-type cell was estimated to be 73 mM by assuming that a *B. subtilis* cell is a cylinder (radius, 0.4 μm; length, 4 μm). This result agrees with the previous observation that the concentration of Mg^{2+} ions, including Mg^{2+} ions chelated in proteins and nucleic acids, in an *E. coli* cell is 90 to 110 mM (55). Surprisingly, the Mg^{2+} content in the Δ*rpmH* cells was significantly lower than that in the wild-type cells. The reduction in Mg^{2+} concentration that was observed in the absence of L34 could be abrogated significantly, although not completely, by the *srh1* suppressor mutation or by the disruption of *yhdP* or overexpression of *mgtE* (Fig. 3). When *yhdP* was disrupted and *mgtE* was overexpressed simultaneously in the Δ*rpmH* mutant, the Mg^{2+} content was almost the same as that of the wild type. Sufficient restoration of the Mg^{2+} content was also observed in the Δ*rpmH srh2* mutant (Fig. 3).

Restoration of the Mg^{2+} concentration suppressed the defect in 70S ribosome formation caused by lack of L34. The elimination of ribosomal protein L34 caused a remarkable reduction in the efficiency of 70S ribosome formation, accompanied by the abnormal accumulation of both 30S and 50S subunits (Fig. 4). It is known that the association of 30S and 50S ribosomal subunits requires Mg^{2+} ions (25–27) and that Mg^{2+} stabilizes the secondary structure of rRNA and the binding of the ribosomal proteins to the rRNA (28–30). These results raise the possibility that restoration of the Mg^{2+} concentration by the disruption of *yhdP* and overexpression of *mgtE* suppresses the defect in 70S ribosome formation that is observed in the Δ*rpmH* mutant. To test this possibility, the ribosome profiles in the Δ*rpmH* mutants after restoration of the cellular Mg^{2+} content by the disruption of *yhdP* and/or overexpression of *mgtE* were examined. Overexpression of MgtE or disruption of YhdP in the Δ*rpmH* mutant partially suppressed the defect in 70S ribosome formation caused by the lack of L34. In contrast, when the *mgtE* gene was overexpressed and the *yhdP* gene was deleted simultaneously in the Δ*rpmH* mutant, 70S ribosome formation occurred almost as efficiently as in the wild type (Fig. 4). To confirm that the restoration of 70S ribosome forma-

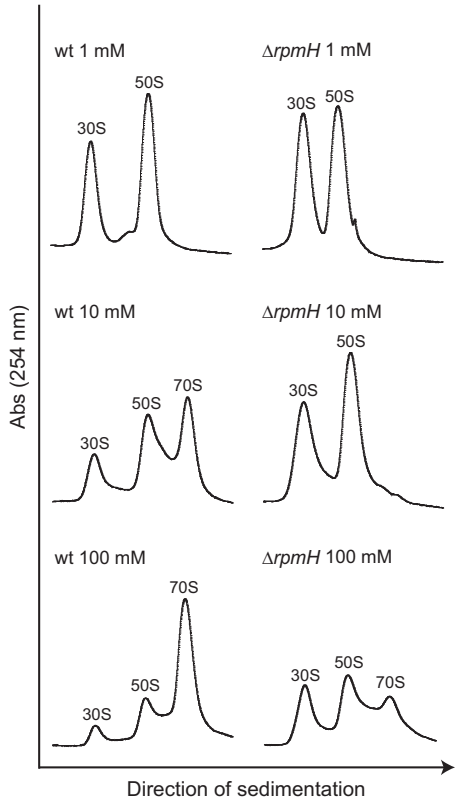

FIG 5 50S subunits lacking L34 form 70S ribosomes *in vitro* at high concentrations of Mg^{2+}. 30S and 50S subunits were prepared from the Δ*rpmH* mutant and wild type, and association experiments were performed at different Mg^{2+} concentrations. The 30S, 50S, and 70S peaks are indicated in each individual profile. wt, wild type; Abs, absorbance.

tion that was observed *in vivo* could be attributed to increases in the concentration of Mg^{2+}, *in vitro* experiments on 70S ribosome formation using ribosomal subunits prepared from the Δ*rpmH* mutant were performed at different Mg^{2+} concentrations (Fig. 5). When the Mg^{2+} concentration in the gradient buffer was 1 mM, 70S ribosomes could not be formed even when the subunits were prepared from wild-type *B. subtilis*. In the presence of 10 mM Mg^{2+}, 30S and 50S subunits prepared from the wild type could form 70S ribosomes, whereas those from the Δ*rpmH* mutant could not. However, in gradient buffer that contained 100 mM Mg^{2+}, a small peak of 70S ribosomes was observed even when the subunits were prepared from the Δ*rpmH* mutant. These results indicate that 50S subunits that lack L34 can interact with 30S subunits and form 70S ribosomes only at high concentrations of Mg^{2+}. Thus, it is probable that increased levels of cellular Mg^{2+} suppress the defect in the formation of 70S ribosomes and the accompanying severe slow-growth phenotype that is caused by lack of ribosomal protein L34.

Correlation between the amount of 70S ribosomes and the content of Mg^{2+} in the cell. Although we assumed that lack of L34 affected the expression of *yhdP* and *mgtE* because decreased levels of Mg^{2+} were observed in the Δ*rpmH* mutant cells, the transcriptional activities of these genes, as well as the amounts of these proteins in the cell, did not differ significantly between the wild type and the Δ*rpmH* mutant (see Table S3 and Fig. S2 in the supplemental material). Consequently, we expected that addition of Mg^{2+} to the medium would suppress the defects observed in the absence of L34. However, the growth rate of the Δ*rpmH* mutant was not restored even if Mg^{2+} was added to the medium at a final concentration of 200 mM (see Fig. S3). Thus, an increase in the environmental concentration of Mg^{2+} could not restore the reduced Mg^{2+} content that resulted from a lack of L34. The content of free Mg^{2+} ions in the cell is maintained at an essentially invariant level by tight regulation of uptake and efflux (56, 57). It has been demonstrated that the cytosolic cystathionine β-synthase (CBS) domain of MgtE in *T. thermophilus* binds specifically to Mg^{2+} and strictly controls the homeostasis of Mg^{2+} in the cell through a conformational change in the transmembrane domain (52–54). Moreover, the expression of *mgtE* is controlled by a Mg^{2+}-responsive riboswitch, which is located in the 5′ leader region of the *mgtE* gene in *B. subtilis* (41). If the concentration of free Mg^{2+} ions in Δ*rpmH* cells is also tightly controlled by the regulation of *mgtE* through the Mg^{2+} riboswitch and by the activity of MgtE, it can be assumed that the reduction in Mg^{2+} content that occurs in the absence of L34 is due to a deficiency in the capacity of the cell to accumulate Mg^{2+}. It is known that the number of ribosomes per cell can vary between 3,000 and 70,000 depending on the growth rate (58). Given the strong evidence that free Mg^{2+} is regulated tightly to between 1 and 5 mM (59, 60), and assuming that the ribosome-bound Mg^{2+} represents a substantial fraction of the total Mg^{2+}, then a variation in the number of 70S ribosomes will have a significant effect on the total Mg^{2+} concentration, which is normally around 110 mM. To test this hypothesis, we determined the Mg^{2+} content in the Δ*rplA* (L1) and Δ*rplW* (L23) mutants, in which the efficiency of 70S ribosome formation is reduced significantly, and found that the lack of ribosomal protein L1 or L23 also decreased the Mg^{2+} content in the cells, as seen in the Δ*rpmH* mutant (Fig. 6A). Indeed, the numbers of 70S ribosomes and polysomes in cells lacking one of these ribosomal proteins were decreased markedly compared with those in wild-type cells when the applied volumes of crude extracts used for the experiment were normalized to the amount of chromosomal DNA as described in Materials and Methods (Fig. 6B). The areas of the peaks that corresponded to the 70S ribosomes and polysomes were 47%, 42%, and 32% of the wild-type area in the Δ*rplA* (L1), Δ*rplW* (L23), and Δ*rpmH* (L34) mutants, respectively. In addition, the total amount of 30S subunits plus 50S subunits plus 70S ribosomes, including polysomes, was decreased slightly in these mutants. When the 50S and 30S subunits were included with the 70S ribosomes and polysomes, the total areas of the peaks were 89%, 77%, and 80% of the wild-type area in the Δ*rplA*, Δ*rplW*, and Δ*rpmH* mutants, respectively. Previously, we have constructed mutants that harbor one to nine copies of the *rrn* operon in their genome (the wild type contains 10 copies) and confirmed that the number of ribosomes is reduced in these mutants, especially in those that harbor only one or two *rrn* operons (61, 62). In the present study, we determined the cellular Mg^{2+} content in these mutants and found that the Mg^{2+} content decreased as the number of *rrn* operons decreased (Fig. 6A). The decrease in the number of *rrn* operons correlated with the reduction in the amount of ribosomes as well as the reduction in the growth rate (61, 62). These results suggest that the Mg^{2+} content in the cell is influenced by the amount of ribosomes present, especially 70S ribosomes and polysomes.

To investigate the effect on cell proliferation of the decrease in 70S ribosomes and concomitant reduction in Mg^{2+} content that

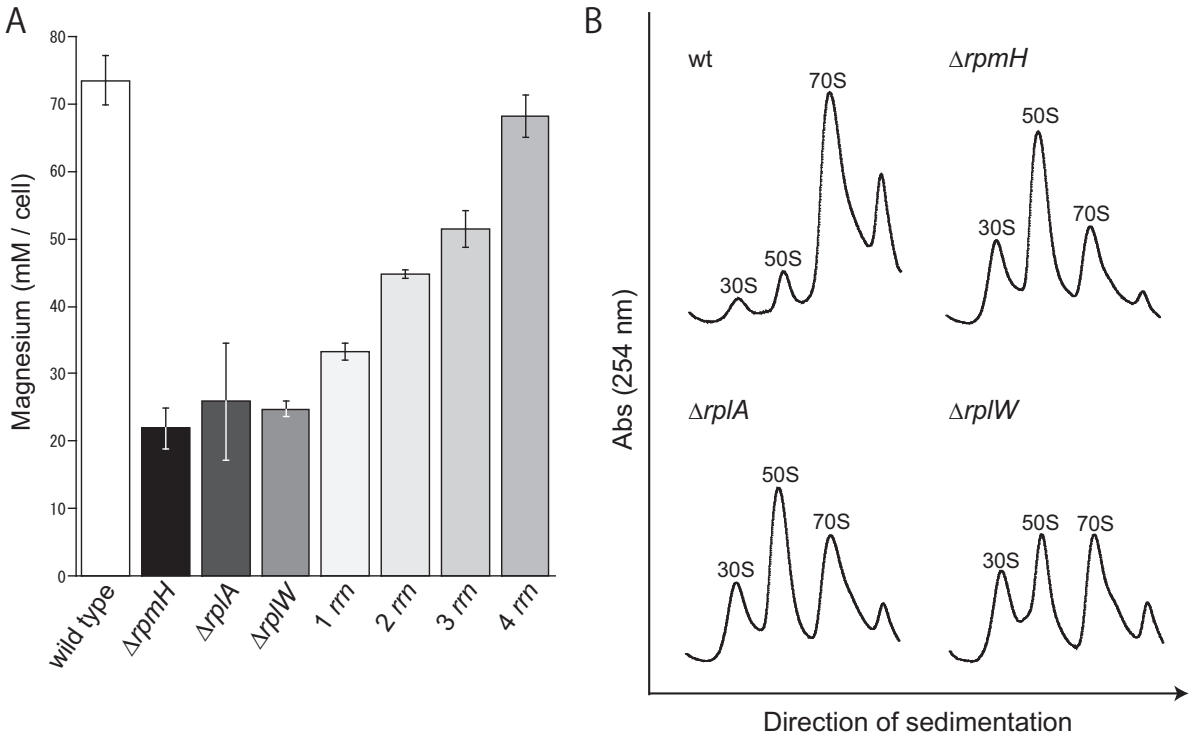

FIG 6 Reduction of the Mg^{2+} content in mutants that contained reduced amounts of 70S ribosomes. (A) The Mg^{2+} content per cell during exponential phase was measured as described in Materials and Methods. The means of three independent experiments are shown. Error bars indicate standard deviations. RIK539 harboring only the *rrnA* operon within the genome is indicated as 1 *rrn*. RIK1754 harboring only the *rrnA* and *rrnI* operons is indicated as 2 *rrn*. RIK1437 harboring only the *rrnA*, *rrnI*, and *rrnO* operons is indicated as 3 *rrn*. RIK1463 harboring only the *rrnA*, *rrnI*, *rrnO*, and *rrnE* operons is indicated as 4 *rrn*. These mutants harboring reduced numbers of the *rrn* operon have been described by Yano et al. (62). (B) Crude cell extracts, whose applied volumes were normalized as described in Materials and Methods, were sedimented through a 10 to 40% sucrose gradient. The 30S, 50S, and 70S peaks are indicated in each individual profile. wt, wild type; Abs, absorbance.

was caused by the lack of L34, growth of the Δ*rpmH* mutant was observed under Mg^{2+}-deficient conditions (Fig. 7). In the MCA medium to which 1 mM $MgSO_4$ had been added, both the wild type and the Δ*rpmH* mutant grew continuously, whereas cell proliferation was limited in the MCA medium to which only 10 μM Mg^{2+} had been added. It should be noted that the standard MCA medium contained 6 μM Mg^{2+}. Under the Mg^{2+}-deficient conditions, a 5.6-fold increase in the OD_{600} value of the wild-type culture was observed whereas the OD_{600} value of the Δ*rpmH* culture increased only 1.9-fold. These results suggest that the initial amount of 70S ribosomes and Mg^{2+} in the cell was an important factor in limiting cell proliferation under Mg^{2+}-deficient conditions.

DISCUSSION

The *rpmH* gene encodes the ribosomal protein L34. Although *rpmH* genes have been cloned from many bacteria owing to their genomic location close to the replication origin (18–22), the function of L34 within the ribosome is not fully understood. In the present study, we characterized the Δ*rpmH* mutant of *B. subtilis* and two suppressor mutants and demonstrated that ribosomal protein L34 is essential for efficient formation of the 70S ribosome. We also showed that its function can be complemented partially by Mg^{2+}. In addition, we obtained results that suggest that the number of 70S ribosomes in a cell influences the cellular Mg^{2+} content.

The defects in the formation of the 70S ribosome and the as-

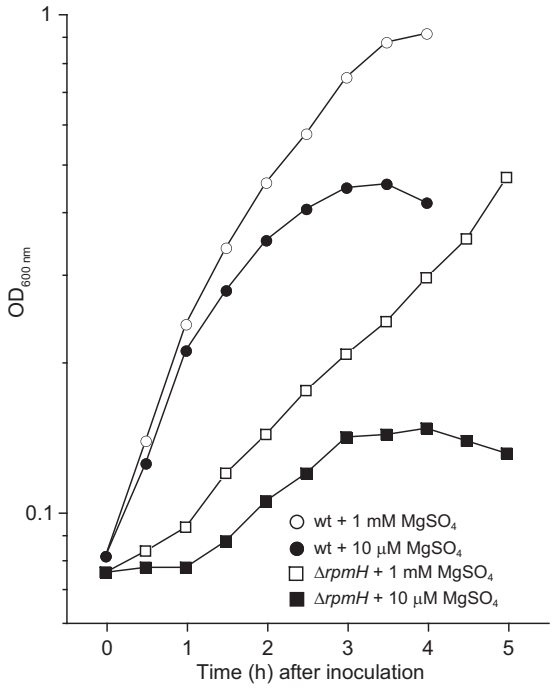

FIG 7 Effect of the lack of L34 on cell proliferation under Mg^{2+}-deficient conditions. Precultured cells were grown at 37°C in minimal medium that contained 1 mM Mg^{2+} or 10 μM Mg^{2+}, and the optical density at 600 nm was measured (see details in Materials and Methods). wt, wild type.

sociated slow-growth phenotype that were observed in the absence of L34 were suppressed by disruption of the *yhdP* gene and overexpression of the *mgtE* gene, which increased the Mg^{2+} content in the cell. Therefore, we predict that the detected insertion and missense mutations in *yhdP* inhibit Mg^{2+} efflux, whereas the missense mutation in *mgtE* promotes Mg^{2+} import. MgtE, a major importer of Mg^{2+} in *B. subtilis*, has been studied in detail, including crystal structure analyses, in *T. thermophilus*. It has been suggested that binding of Mg^{2+} to the cytosolic CBS domain of the MgtE dimer alters the orientation of the plug helices, which comprise long helices that connect the CBS and transmembrane domains, and limits the import of Mg^{2+} into the cell by controlling the gating of the ion-conducting pore in the transmembrane domains (52–54). The predicted structure of *B. subtilis* MgtE suggests that Ala266, which is mutated to Val in the Δ*rpmH srh2* mutant, is located in the connecting region between the plug helix and transmembrane domain (see Fig. S4 in the supplemental material). Therefore, it is likely that the A226V mutation affects the change in orientation of the plug helix and associated closing of the transmembrane domains that occur upon Mg^{2+} binding and facilitate the transport of Mg^{2+} into the cell. It is difficult to infer the effect that the mutations in YhdP have on the conformation of the protein because no crystal structures of YhdP homologues are available. However, the mutations in the *yhdP* gene that were found in both the Δ*rpmH srh1* and Δ*rpmH srh2* suppressor mutants must destroy the function of YhdP because they suppressed the defects caused by lack of L34, similarly to disruption of *yhdP*, which restored the Mg^{2+} content in the Δ*rpmH* cell. These results, together with the observation that overexpression of *yhdP* exacerbated the low growth rate in the Δ*rpmH* mutant, strongly suggest that YhdP is an efflux pump for Mg^{2+} in *B. subtilis*.

We found that L34 is essential for efficient interaction between the 30S and 50S subunits, even though the location of L34 within the ribosome is far from the region of interaction of the two subunits (8). In the 50S fraction from the Δ*rpmH* mutant, the amount of ribosomal protein L16 was reduced significantly in addition to the lack of L34 (see Fig. S5A in the supplemental material). We expect that the lack of L34 reduces the binding affinity of L16 for the 50S subunit, probably due to a conformational change in the 50S subunit. In the ribosome, L16 is located near the region of interaction of the two subunits and is inserted between two stems of the 23S rRNA, helix 38 and helix 89 (8, 63). Given that helix 38 is known to form an intersubunit bridge in the 70S structure (8, 63), lack of L16 probably causes a defect in the formation of the 70S ribosome. In fact, it has been reported that incorporation of L16 induces a strong conformational change in 50S particles and influences the association of the ribosomal subunits (64, 65). Similarly, we have reported recently that the H142L mutation in ribosomal protein L2 not only reduces the efficiency of formation of the 70S ribosome but also leads to a deficiency of L16 in the 50S subunit (48). Therefore, it seems that the defect in formation of the 70S ribosome in the Δ*rpmH* mutant is probably due to conformational changes in the 50S subunit that are caused by lack of L34 followed by a reduction in the binding affinity of L16.

A key question is how the restoration of Mg^{2+} content suppressed the defect in 70S ribosome formation caused by lack of L34. One probable reason is stabilization of the 50S subunit. Mg^{2+} stabilizes the binding of ribosomal proteins to the rRNA and the secondary structure of rRNA in the ribosome (28–30). Moreover, it has been demonstrated that Mg^{2+} concentration controls the dynamics of the ribosome exquisitely through altering ribosome stability and flexibility (66). Therefore, it seems likely that the restoration of Mg^{2+} content in the cell enables the normal rRNA structure to form and L16 to bind to the 50S subunit, which improves the conformational stability of 50S subunits that lack L34 and in turn restores formation of the 70S ribosome. In fact, the ribosome fractions that were prepared from the Δ*rpmH* mutant after restoration of the Mg^{2+} content by disruption of YhdP and overexpression of MgtE contained considerable amounts of L16 (see Fig. S5B in the supplemental material). Another possible reason for why Mg^{2+} improves the efficiency of 70S ribosome formation in the absence of L34 is increased stabilization of the intersubunit bridges. It is known that the *in vitro* association of the 30S and 50S ribosomal subunits depends strongly on the Mg^{2+} concentration (25–27) and that at least 5 of the 12 subunit bridges that exist between different ribosomal components are stabilized by Mg^{2+} (8, 67). Therefore, in the Δ*rpmH* mutant, restoration of the Mg^{2+} content probably improved the efficiency of 70S ribosome formation by stabilizing both the conformation of the 50S subunit and the intersubunit bridges (Fig. 8). It should be noted that the decrease in growth rate of the Δ*rplW* mutant, in which the efficiency of 70S ribosome formation is decreased significantly, was partially suppressed by the overexpression of MgtE, probably due to the restoration of 70S ribosome formation (see Fig. S6A in the supplemental material). In contrast, the growth rate of the Δ*rplA* mutant was not restored by overexpression of MgtE (see Fig. S6B in the supplemental material). The fact that the growth rate was not restored even when 70S formation was restored by an increase in Mg^{2+} can be explained by the fact that ribosomal protein L1,

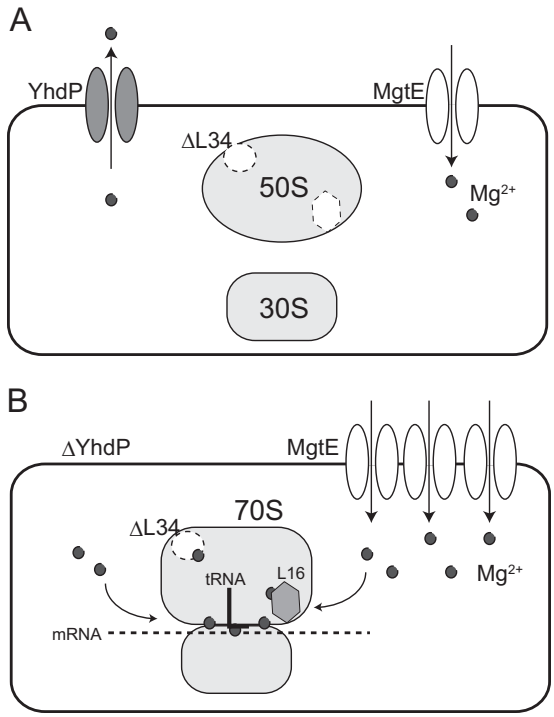

FIG 8 Mechanism of suppression in mutant lacking L34 through disruption of *yhdP* and overexpression of *mgtE*. (A) Defect in formation of 70S ribosome followed by reduction of Mg^{2+} content in the absence of L34. (B) Restoration of Mg^{2+} content and of 70S ribosome formation by disruption of *yhdP* and overexpression of *mgtE* in the Δ*rpmH* mutant. See the text for details.

which is localized to the stalk region near the E site (8, 68), plays a critical role in protein synthesis in terms of the translocation of the newly deacylated tRNA from the P to the E site (69). At a high concentration of Mg^{2+}, 50S subunits that lacked L34 could form 70S ribosomes even in the *in vitro* association experiments (Fig. 5). The concentration of free Mg^{2+} in *E. coli* and *Salmonella enterica*, not including Mg^{2+} ions chelated in proteins and nucleic acids, has been estimated experimentally to be between 1 and 5 mM (59, 60). Given that the Mg^{2+} concentration that allowed formation of the 70S peak from subunits prepared from the Δ*rpmH* mutant under *in vitro* conditions was extremely high (100 mM) compared with the concentration of free Mg^{2+} in the cell, the 50S subunit presumably interacted with the 30S subunit through intersubunit bridges that do not depend on L34 or L16 *in vitro*. However, these 70S ribosomes, whose conformation can be maintained only under limited conditions, may be unstable. 70S ribosomes were not formed sufficiently *in vitro*, even at the extremely high (100 mM) concentration of Mg^{2+}, because ribosomal protein L16 was not supplied to ribosome subunits prepared from the Δ*rpmH* mutant. However, the restoration of 70S ribosome formation that was observed when the *mgtE* gene was overexpressed in the Δ*rpmH* mutant with the *yhdP* deletion was probably due to elevation of the free Mg^{2+} concentration in the cell.

In the Δ*rpmH* mutant, a reduction in the cellular Mg^{2+} content was also observed (Fig. 3). The probable reasons for this reduction are (i) a decrease in the amount of 70S ribosomes, (ii) a decrease in the amount of protein and RNA other than ribosomes that can chelate Mg^{2+}, and (iii) a reduction in the free Mg^{2+} content in the cell. The ribosome has the highest capacity of any macromolecule in the cell for binding Mg^{2+}, with more than 170 Mg^{2+} ions per complex (70). These 170 Mg^{2+} ions bound to the 70S ribosome were detected with particularly high B factors and thus did not include Mg^{2+} ions that were associated loosely or only through outer-sphere interactions. Therefore, the 70S ribosome probably contains many more Mg^{2+} ions than reported previously. Given that *E. coli* growing in exponential phase contains approximately 70,000 ribosomes per cell (58), a large amount of Mg^{2+} is probably sequestered in the 70S ribosomes. Indeed, we found that, in addition to the Δ*rpmH* mutant, the Mg^{2+} content was also reduced in other mutants that contained significantly decreased amounts of 70S ribosomes, such as disruptants of ribosomal-protein genes and strains with a reduced number of *rrn* operons (Fig. 6). The difference in the areas of the peaks between the Δ*rpmH* mutant and the wild type was greater when only the 70S ribosomes and polysomes were considered (the mutant was 32% of the wild-type value) than when the 30S and 50S subunits were included as well (the mutant was 80% of the wild-type value). Therefore, it is likely that the decrease in cellular Mg^{2+} content observed in the mutant analyzed in the present study is caused by a reduction in the level of 70S ribosomes and polysomes rather than a reduction in the total amount of available 30S and 50S subunits. Given that Mg^{2+} is also involved in the stabilization of both tRNA binding and intersubunit bridges in translating 70S ribosomes (32–34, 67, 71), the total amount of Mg^{2+} that is contained in 70S ribosomes and polysomes is greater than that contained in the equivalent amount of individual ribosome subunits. In addition, the binding capacity of 50S subunits that lack L34 and L16 for Mg^{2+} is probably lower than that of intact 50S subunits. Consequently, we predict that the decrease in the amount of Mg^{2+} ions is much greater than that due simply to the reduction in number of ribosome subunits that is caused by the lack of L34. Moreover, it has been reported previously that the amount of Mg^{2+} in the ribosome fraction is influenced by the concentration of Mg^{2+} in the culture medium (72) and that ribosome flexibility is controlled by Mg^{2+} concentration (66). Thus, the amount of Mg^{2+} in the 70S ribosome might vary. The second probable reason why the absence of L34 caused a reduction in the Mg^{2+} content is a decrease in the amount of protein and RNA in general that can chelate Mg^{2+}. A decrease in the amount of 70S ribosomes and the consequent reduction in translation activity in a cell causes a reduction in the growth rate and in the total amount of protein and RNA, including that which can chelate Mg^{2+}. The reduction in these chelating agents might decrease the cellular Mg^{2+} content. The final probable reason is a decrease in the free Mg^{2+} content in the cell. However, as described previously, the concentration of free Mg^{2+} is controlled tightly (59, 60). Given that the level of expression of MgtE, a major transporter of Mg^{2+} in *B. subtilis*, was not changed significantly in the Δ*rpmH* mutant compared with the wild type (see Table S3 and Fig. S2 in the supplemental material), the concentration of free Mg^{2+} in Δ*rpmH* cells might not decrease drastically. However, the possibility remains that a defect occurs in an alternative route of Mg^{2+} transport, for example, via YfjQ. Although we cannot fully explain at present the mechanism by which the absence of L34 causes a reduction in the Mg^{2+} content, the restoration of Mg^{2+} content in the Δ*rpmH* mutant by the disruption of *yhdP* and overexpression of *mgtE* might be caused by an increase in the free Mg^{2+} concentration followed by a subsequent increase in the amount of 70S ribosomes, as illustrated in Fig. 8.

When sufficient cellular reserves of 70S ribosomes and Mg^{2+} are available, the cells can adapt to environmental changes such as a decrease in Mg^{2+} concentration to some extent. When the Mg^{2+} concentration in the culture medium was decreased, the wild-type cells could proliferate three times as much as the Δ*rpmH* mutant, which did not contain sufficient 70S ribosomes and Mg^{2+} (Fig. 7). Given that the synthesis of 70S ribosomes, which requires Mg^{2+}, is probably difficult under Mg^{2+}-deficient conditions, the amount of 70S ribosomes and Mg^{2+} in the cell is reduced further by cell division under such conditions. In fact, the depletion of ribosomes is observed under Mg^{2+}-deficient conditions in *E. coli* (73). Therefore, ribosomal proteins such as L34 play important roles in ensuring not only efficient cell proliferation but also cell survival in an environment with a limited concentration of Mg^{2+}.

The finding that the function of ribosomal protein L34, which is required for efficient 70S ribosome formation, can be complemented partially by Mg^{2+} reemphasizes the importance of Mg^{2+} for the conformational stability of the ribosome. In addition, we obtained results that suggest that the amount of 70S ribosomes influences the Mg^{2+} content in the cell. Further investigations should reveal whether, under Mg^{2+}-deficient conditions, the 70S ribosome, which binds a large number of Mg^{2+} ions, can donate Mg^{2+} to enzymes that require the ion for activation.

ACKNOWLEDGMENTS

This work was supported in part by Grants-in-Aid for Scientific Research (C) (G.A.) from the Ministry of Education, Culture, Sports, Science, and Technology of Japan and by the MEXT-Supported Program for the Strategic Research Foundation at Private Universities (S0801025) (http://www.jsps.go.jp/english/index.html).

REFERENCES

1. **Kurland CG.** 1972. Structure and function of the bacterial ribosome. Annu. Rev. Biochem. **41:**377–408. http://dx.doi.org/10.1146/annurev.bi.41.070172.002113.
2. **Nomura M.** 1970. Bacterial ribosome. Bacteriol. Rev. **34:**228–277.
3. **Gao YG, Selmer M, Dunham CM, Weixlbaumer A, Kelley AC, Ramakrishnan V.** 2009. The structure of the ribosome with elongation factor G trapped in the posttranslocational state. Science **326:**694–699. http://dx.doi.org/10.1126/science.1179709.
4. **Nissen P, Hansen J, Ban N, Moore PB, Steitz TA.** 2000. The structural basis of ribosome activity in peptide bond synthesis. Science **289:**920–930. http://dx.doi.org/10.1126/science.289.5481.920.
5. **Ogle JM, Brodersen DE, Clemons WM, Tarry MJ, Carter AP, Ramakrishnan V.** 2001. Recognition of cognate transfer RNA by the 30S ribosomal subunit. Science **292:**897–902. http://dx.doi.org/10.1126/science.1060612.
6. **Schmeing TM, Ramakrishnan V.** 2009. What recent ribosome structures have revealed about the mechanism of translation. Nature **461:**1234–1242. http://dx.doi.org/10.1038/nature08403.
7. **Schmeing TM, Voorhees RM, Kelley AC, Gao YG, Murphy FV, Weir JR, Ramakrishnan V.** 2009. The crystal structure of the ribosome bound to EF-Tu and aminoacyl-tRNA. Science **326:**688–694. http://dx.doi.org/10.1126/science.1179700.
8. **Yusupov MM, Yusupova GZ, Baucom A, Lieberman K, Earnest TN, Cate JH, Noller HF.** 2001. Crystal structure of the ribosome at 5.5 Å resolution. Science **292:**883–896. http://dx.doi.org/10.1126/science.1060089.
9. **Diedrich G, Spahn CM, Stelzl U, Schafer MA, Wooten T, Bochkariov DE, Cooperman BS, Traut RR, Nierhaus KH.** 2000. Ribosomal protein L2 is involved in the association of the ribosomal subunits, tRNA binding to A and P sites and peptidyl transfer. EMBO J. **19:**5241–5250. http://dx.doi.org/10.1093/emboj/19.19.5241.
10. **Khaitovich P, Mankin AS, Green R, Lancaster L, Noller HF.** 1999. Characterization of functionally active subribosomal particles from *Thermus aquaticus*. Proc. Natl. Acad. Sci. U. S. A. **96:**85–90. http://dx.doi.org/10.1073/pnas.96.1.85.
11. **Schulze H, Nierhaus KH.** 1982. Minimal set of ribosomal components for reconstitution of the peptidyltransferase activity. EMBO J. **1:**609–613.
12. **Uhlein M, Weglöhner W, Urlaub H, Wittmann-Liebold B.** 1998. Functional implications of ribosomal protein L2 in protein biosynthesis as shown by *in vivo* replacement studies. Biochem. J. **331:**423–430.
13. **Willumeit R, Forthmann S, Beckmann J, Diedrich G, Ratering R, Stuhrmann HB, Nierhaus KH.** 2001. Localization of the protein L2 in the 50S subunit and the 70S *E. coli* ribosome. J. Mol. Biol. **305:**167–177. http://dx.doi.org/10.1006/jmbi.2000.4289.
14. **Roberts E, Sethi A, Montoya J, Woese CR, Luthey-Schulten Z.** 2008. Molecular signatures of ribosomal evolution. Proc. Natl. Acad. Sci. U. S. A. **105:**13953–13958. http://dx.doi.org/10.1073/pnas.0804861105.
15. **Baba T, Ara T, Hasegawa M, Takai Y, Okumura Y, Baba M, Datsenko KA, Tomita M, Wanner BL, Mori H.** 2006. Construction of *Escherichia coli* K-12 in-frame, single-gene knockout mutants: the Keio collection. Mol. Syst. Biol. **2:**2006.0008. http://dx.doi.org/10.1038/msb4100050.
16. **Shoji S, Dambacher CM, Shajani Z, Williamson JR, Schultz PG.** 2011. Systematic chromosomal deletion of bacterial ribosomal protein genes. J. Mol. Biol. **413:**751–761. http://dx.doi.org/10.1016/j.jmb.2011.09.004.
17. **Akanuma G, Nanamiya H, Natori Y, Yano K, Suzuki S, Omata S, Ishizuka M, Sekine Y, Kawamura F.** 2012. Inactivation of ribosomal protein genes in *Bacillus subtilis* reveals importance of each ribosomal protein for cell proliferation and cell differentiation. J. Bacteriol. **194:**6282–6291. http://dx.doi.org/10.1128/JB.01544-12.
18. **Calcutt MJ, Schmidt FJ.** 1992. Conserved gene arrangement in the origin region of the Streptomyces coelicolor chromosome. J. Bacteriol. **174:**3220–3226.
19. **Fujita MQ, Yoshikawa H, Ogasawara N.** 1990. Structure of the *dnaA* region of *Micrococcus luteus*: conservations and variations among eubacteria. Gene **93:**73–78. http://dx.doi.org/10.1016/0378-1119(90)90138-H.
20. **Hansen FG, Hansen EB, Atlung T.** 1982. The nucleotide sequence of the *dnaA* gene promoter and of the adjacent *rpmH* gene, coding for the ribosomal protein L34, of *Escherichia coli*. EMBO J. **1:**1043–1048.
21. **Moriya S, Ogasawara N, Yoshikawa H.** 1985. Structure and function of the region of the replication origin of the *Bacillus subtilis* chromosome. III. Nucleotide sequence of some 10,000 base pairs in the origin region. Nucleic Acids Res. **13:**2251–2265.
22. **Old IG, Margarita D, Saint Girons I.** 1992. Nucleotide sequence of the *Borrelia burgdorferi rpmH* gene encoding ribosomal protein L34. Nucleic Acids. Res. **20:**6097. http://dx.doi.org/10.1093/nar/20.22.6097.
23. **Herold M, Nierhaus KH.** 1987. Incorporation of six additional proteins to complete the assembly map of the 50 S subunit from *Escherichia coli* ribosomes. J. Biol. Chem. **262:**8826–8833.
24. **Panagiotidis CA, Huang SC, Canellakis ES.** 1995. Relationship of the expression of the S20 and L34 ribosomal proteins to polyamine biosynthesis in *Escherichia coli*. Int. J. Biochem. Cell Biol. **27:**157–168. http://dx.doi.org/10.1016/1357-2725(94)00068-M.
25. **Blaha G, Burkhardt N, Nierhaus KH.** 2002. Formation of 70S ribosomes: large activation energy is required for the adaptation of exclusively the small ribosomal subunit. Biophys. Chem. **96:**153–161. http://dx.doi.org/10.1016/S0301-4622(02)00021-2.
26. **Liiv A, O'Connor M.** 2006. Mutations in the intersubunit bridge regions of 23 S rRNA. J. Biol. Chem. **281:**29850–29862. http://dx.doi.org/10.1074/jbc.M603013200.
27. **Tissieres A, Watson JD, Schlessinger D, Hollingworth BR.** 1959. Ribonucleoprotein particles from *Escherichia coli*. J. Mol. Biol. **1:**221–233. http://dx.doi.org/10.1016/S0022-2836(59)80029-2.
28. **Drygin D, Zimmermann RA.** 2000. Magnesium ions mediate contacts between phosphoryl oxygens at positions 2122 and 2176 of the 23S rRNA and ribosomal protein L1. RNA. **6:**1714–1726. http://dx.doi.org/10.1017/S1355838200001436.
29. **Klein DJ, Moore PB, Steitz TA.** 2004. The contribution of metal ions to the structural stability of the large ribosomal subunit. RNA **10:**1366–1379. http://dx.doi.org/10.1261/rna.7390804.
30. **Petrov AS, Bernier CR, Hsiao C, Okafor CD, Tannenbaum E, Stern J, Gaucher E, Schneider D, Hud NV, Harvey SC, Williams LD.** 2012. RNA-magnesium-protein interactions in large ribosomal subunit. J. Phys. Chem. B **116:**8113–8120. http://dx.doi.org/10.1021/jp304723w.
31. **Hirokawa G, Kiel MC, Muto A, Kawai G, Igarashi K, Kaji H, Kaji A.** 2002. Binding of ribosome recycling factor to ribosomes, comparison with tRNA. J. Biol. Chem. **277:**35847–35852. http://dx.doi.org/10.1074/jbc.M206295200.
32. **Kirillov SV, Semenkov YP.** 1982. Non-exclusion principle of Ac-Phe-tRNAPhe interaction with the donor and acceptor sites of *Escherichia coli* ribosomes. FEBS Lett. **148:**235–238. http://dx.doi.org/10.1016/0014-5793(82)80814-4.
33. **Konevega AL, Soboleva NG, Makhno VI, Semenkov YP, Wintermeyer W, Rodnina MV, Katunin VI.** 2004. Purine bases at position 37 of tRNA stabilize codon-anticodon interaction in the ribosomal A site by stacking and Mg^{2+}-dependent interactions. RNA **10:**90–101. http://dx.doi.org/10.1261/rna.5142404.
34. **Selmer M, Dunham CM, Murphy FV, Weixlbaumer A, Petry S, Kelley AC, Weir JR, Ramakrishnan V.** 2006. Structure of the 70S ribosome complexed with mRNA and tRNA. Science **313:**1935–1942. http://dx.doi.org/10.1126/science.1131127.
35. **Cowan JA.** 2002. Structural and catalytic chemistry of magnesium dependent enzymes. Biometals **15:**225–235. http://dx.doi.org/10.1023/A:1016022730880.
36. **Hartwig A.** 2001. Role of magnesium in genomic stability. Mutat. Res. **475:**113–121. http://dx.doi.org/10.1016/S0027-5107(01)00074-4.
37. **Sambrook J, Fritsch EF, Maniatis T.** 1989. Molecular cloning: a laboratory manual, 2nd ed. Cold Spring Harbor Laboratory Press, Cold Spring Harbor, NY.
38. **Ashikaga S, Nanamiya H, Ohashi Y, Kawamura F.** 2000. Natural genetic competence in *Bacillus subtilis* natto OK2. J. Bacteriol. **182:**2411–2415. http://dx.doi.org/10.1128/JB.182.9.2411-2415.2000.
39. **Anagnostopoulos C, Spizizen J.** 1961. Requirements for transformation in *Bacillus subtilis*. J. Bacteriol. **81:**741–746.
40. **Joseph P, Fantino JR, Herbaud ML, Denizot F.** 2001. Rapid orientated cloning in a shuttle vector allowing modulated gene expression in *Bacillus subtilis*. FEMS Microbiol. Lett. **205:**91–97. http://dx.doi.org/10.1111/j.1574-6968.2001.tb10930.x.
41. **Dann CE, III, Wakeman CA, Sieling CL, Baker SC, Irnov I, Winkler WC.** 2007. Structure and mechanism of a metal-sensing regulatory RNA. Cell **130:**878–892. http://dx.doi.org/10.1016/j.cell.2007.06.051.
42. **Imamura D, Kobayashi K, Sekiguchi J, Ogasawara N, Takeuchi M, Sato T.** 2004. *spoIVH* (*ykvV*), a requisite cortex formation gene, is expressed in both sporulating compartments of *Bacillus subtilis*. J. Bacteriol. **186:**5450–5459. http://dx.doi.org/10.1128/JB.186.16.5450-5459.2004.
43. **Li H, Handsaker B, Wysoker A, Fennell T, Ruan J, Homer N, Marth**

G, Abecasis G, Durbin R, 1000 Genome Project Data Processing Subgroup. 2009. The Sequence Alignment/Map (SAM) format and SAMtools. Bioinformatics **25:**2078–2079. http://dx.doi.org/10.1093/bioinformatics/btp352.

44. **Li H, Durbin R.** 2009. Fast and accurate short read alignment with Burrows-Wheeler transform. Bioinformatics **25:**1754–1760. http://dx.doi.org/10.1093/bioinformatics/btp324.
45. **Chen K, Wallis JW, McLellan MD, Larson DE, Kalicki JM, Pohl CS, McGrath SD, Wendl MC, Zhang Q, Lock DP, Shi X, Fulton RS, Ley TJ, Wilson RK, Ding L, Mardis ER.** 2009. BreakDancer: an algorithm for high-resolution mapping of genomic structural variation. Nat. Methods **6:**677–681. http://dx.doi.org/10.1038/nmeth.1363.
46. **Robinson JT, Thorvaldsdóttir H, Winckler W, Guttman M, Lander ES, Getz G, Mesirov JP.** 2011. Integrative genomics viewer. Nat. Biotechnol. **29:**24–26. http://dx.doi.org/10.1038/nbt.1754.
47. **Natori Y, Nanamiya H, Akanuma G, Kosono S, Kudo T, Ochi K, Kawamura F.** 2007. A fail-safe system for the ribosome under zinc-limiting conditions in *Bacillus subtilis*. Mol. Microbiol. **63:**294–307. http://dx.doi.org/10.1111/j.1365-2958.2006.05513.x.
48. **Suzuki S, Tanigawa O, Akanuma G, Nanamiya H, Kawamura F, Tagami K, Nomura N, Kawabata T, Sekine Y.** 2014. Enhanced expression of *Bacillus subtilis yaaA* can restore both the growth and sporulation defects caused by mutation of *rplB*, encoding ribosomal protein L2. Microbiology **160:**1040–1053. http://dx.doi.org/10.1099/mic.0.076463-0.
49. **Nanamiya H, Akanuma G, Natori Y, Murayama R, Kosono S, Kudo T, Kobayashi K, Ogasawara N, Park SM, Ochi K, Kawamura F.** 2004. Zinc is a key factor in controlling alternation of two types of L31 protein in the *Bacillus subtilis* ribosome. Mol. Microbiol. **52:**273–283. http://dx.doi.org/10.1111/j.1365-2958.2003.03972.x.
50. **Wada A.** 1986. Analysis of *Escherichia coli* ribosomal proteins by an improved two dimensional gel electrophoresis. I. Detection of four new proteins. J. Biochem. **100:**1583–1594.
51. **Gibson MM, Bagga DA, Miller CG, Maguire ME.** 1991. Magnesium transport in *Salmonella typhimurium*: the influence of new mutations conferring Co^{2+} resistance on the CorA Mg^{2+} transport system. Mol. Microbiol. **5:**2753–2762. http://dx.doi.org/10.1111/j.1365-2958.1991.tb01984.x.
52. **Hattori M, Iwase N, Furuya N, Tanaka Y, Tsukazaki T, Ishitani R, Maguire ME, Ito K, Maturana A, Nureki O.** 2009. Mg^{2+}-dependent gating of bacterial MgtE channel underlies Mg^{2+} homeostasis. EMBO J. **28:**3602–3612. http://dx.doi.org/10.1038/emboj.2009.288.
53. **Hattori M, Tanaka Y, Fukai S, Ishitani R, Nureki O.** 2007. Crystal structure of the MgtE Mg^{2+} transporter. Nature **448:**1072–1075. http://dx.doi.org/10.1038/nature06093.
54. **Ishitani R, Sugita Y, Dohmae N, Furuya N, Hattori M, Nureki O.** 2008. Mg^{2+}-sensing mechanism of Mg^{2+} transporter MgtE probed by molecular dynamics study. Proc. Natl. Acad. Sci. U. S. A. **105:**15393–15398. http://dx.doi.org/10.1073/pnas.0802991105.
55. **Moncany ML, Kellenberger E.** 1981. High magnesium content of *Escherichia coli* B. Experientia **37:**846–847. http://dx.doi.org/10.1007/BF01985672.
56. **O'Connor K, Fletcher SA, Csonka LN.** 2009. Increased expression of Mg^{2+} transport proteins enhances the survival of *Salmonella enterica* at high temperature. Proc. Natl. Acad. Sci. U. S. A. **106:**17522–17527. http://dx.doi.org/10.1073/pnas.0906160106.
57. **Silver S, Clark D.** 1971. Magnesium transport in *Escherichia coli*. J. Biol. Chem. **246:**569–576.
58. **Kaczanowska M, Rydén-Aulin M.** 2007. Ribosome biogenesis and the translation process in *Escherichia coli*. Microbiol. Mol. Biol. Rev. **71:**477–494. http://dx.doi.org/10.1128/MMBR.00013-07.
59. **Alatossava T, Jutte H, Kuhn A, Kellenberger E.** 1985. Manipulation of intracellular magnesium content in polymyxin B nonapeptide-sensitized *Escherichia coli* by ionophore A23187. J. Bacteriol. **162:**413–419.
60. **Froschauer EM, Kolisek M, Dieterich F, Schweigel M, Schweyen RJ.** 2004. Fluorescence measurements of free $[Mg^{2+}]$ by use of mag-fura 2 in *Salmonella enterica*. FEMS Microbiol. Lett. **237:**49–55. http://dx.doi.org/10.1016/j.femsle.2004.06.013.
61. **Nanamiya H, Sato M, Masuda K, Sato M, Wada T, Suzuki S, Natori Y, Katano M, Akanuma G, Kawamura F.** 2010. *Bacillus subtilis* mutants harbouring a single copy of the rRNA operon exhibit sever defects in growth and sporulation. Microbiology **156:**2944–2952. http://dx.doi.org/10.1099/mic.0.035295-0.
62. **Yano K, Wada T, Suzuki S, Tagami K, Matsumoto T, Shiwa Y, Ishige T, Kawaguchi Y, Masuda K, Akanuma G, Nanamiya H, Niki H, Yoshikawa H, Kawamura F.** 2013. Multiple rRNA operons are essential for efficient cell growth and sporulation as well as outgrowth in *Bacillus subtilis*. Microbiology **159:**2225–2236. http://dx.doi.org/10.1099/mic.0.067025-0.
63. **Harms J, Schluenzen F, Zarivach R, Bashan A, Gat S, Agmon I, Bartels H, Franceschi F, Yonath A.** 2001. High resolution structure of the large ribosomal subunit from a mesophilic eubacterium. Cell **107:**679–688. http://dx.doi.org/10.1016/S0092-8674(01)00546-3.
64. **Teraoka H, Nierhaus KH.** 1978. Protein L16 induces a conformational change when incorporated into a L16-deficient core derived from *Escherichia coli* ribosomes. FEBS Lett. **88:**223–226. http://dx.doi.org/10.1016/0014-5793(78)80179-3.
65. **Kazemie M.** 1975. The importance of *Escherichia coli* ribosomal proteins L1, L11 and L16 for the association of ribosomal subunits and the formation of the 70-S initiation complex. Eur. J. Biochem. **58:**501–510. http://dx.doi.org/10.1111/j.1432-1033.1975.tb02398.x.
66. **Yamamoto T, Shimizu Y, Ueda T, Shiro Y.** 2010. Mg^{2+} dependence of 70 S ribosomal protein flexibility revealed by hydrogen/deuterium exchange and mass spectrometry. J. Biol. Chem. **285:**5646–5652. http://dx.doi.org/10.1074/jbc.M109.081836.
67. **Liljas A.** 2006. Deepening ribosomal insights. ACS Chem. Biol. **1:**567–569. http://dx.doi.org/10.1021/cb600407u.
68. **Agrawal RK, Lata RK, Frank J.** 1999. Conformational variability in *Escherichia coli* 70S ribosome as revealed by 3D cryo-electron microscopy. Int. J. Biochem. Cell Biol. **31:**243–254. http://dx.doi.org/10.1016/S1357-2725(98)00149-6.
69. **Fei J, Kosuri P, MacDougall DD, Gonzalez RL.** 2008. Coupling of ribosomal L1 stalk and tRNA dynamics during translation elongation. Mol. Cell **30:**348–359. http://dx.doi.org/10.1016/j.molcel.2008.03.012.
70. **Schuwirth BS, Borovinskaya MA, Hau CW, Zhang W, Vila-Sanjurjo A, Holton JM, Cate JH.** 2005. Structures of the bacterial ribosome at 3.5 A resolution. Science **310:**827–834. http://dx.doi.org/10.1126/science.1117230.
71. **Semenkov YP, Rodnina MV, Wintermeyer W.** 2000. Energetic contribution of tRNA hybrid state formation to translocation catalysis on the ribosome. Nat. Struct. Biol. **7:**1027–1031. http://dx.doi.org/10.1038/80938.
72. **Hurwitz C, Rosano CL.** 1967. The intracellular concentration of bound and unbound magnesium ions in *Escherichia coli*. J. Biol. Chem. **242:**3719–3722.
73. **McCarthy BJ.** 1962. Effects of magnesium starvation on ribosome content of *Escherichia coli*. Biochim. Biophys. Acta **55:**880–888. http://dx.doi.org/10.1016/0006-3002(62)90901-0.
74. **Wakeman CA, Goodson JR, Zacharia VM, Winkler WC.** 2014. Assessment of the requirements for magnesium transporters in *Bacillus subtilis*. J. Bacteriol. **196:**1206–1214. http://dx.doi.org/10.1128/JB.01238-13.